Biointerface Research in Applied Chemistry
Open-Access Journal (ISSN: 2069-5837)

Article
Volume 14, Issue 1, 2024, 11
https://doi.org/10.33263/BRIAC141.011

Silver Nanosphere/Polycaprolactone Coated Cotton Fabrics as Hygienic Textiles for Health Care Industries

Sagayanathan Antinate Shilpa [1], Chandramouli Arthi [1,2], Gnanadhas Sobhin Hikku [1,*], Kadarkaraithangam Jeyasubramanian [3], Pandiyarasan Veluswamy [4,5], Hiroya Ikeda [5]

1 Medical Bionanotechnology, Faculty of Allied Health Sciences, Chettinad Hospital and Research Institute, Chettinad Academy of Research and Education (CARE), Kelambakkam, Chennai-603103, India
2 Centre for Nanoscience and Technology, Amrita Vishwa Vidyapeetham, Cochin-682041, Kerala, India
3 Department of Chemistry, Mepco Schlenk Engineering College, Sivakasi, Tamilnadu, India
4 Department of Electronics and Communication Engineering, Indian Institute of Information Technology Design and Manufacturing, Kancheepuram Chennai 600127, India
5 Research Institute of Electronics, Shizuoka University, Hamamatsu 4328011, Japan.
* Correspondence: gshikku@gmail.com (G.S.H.);

Scopus Author ID 56868569200
Received: 23.12.2022; Accepted: 23.02.2023; Published: 2.02.2024

Abstract: Silver nanospheres (Ag NS) of size ranging from ~20 nm are prepared via a green synthesis route employing leaf extract of Maranta arundinaceae as a reducing and capping agent. The prepared Ag NS is conjugated with commercial cotton fabric using polycaprolactone (PCL) as a hydrophobic binder to enable hygienic antibacterial properties through a facile two-step dip-coating technique, followed by air drying. The surface-modified fabric displays antibacterial activity against gram-negative *Escherichia coli* and gram-positive *Staphylococcus epidermidis* and *Methicillin-resistant Staphylococcus aureus bacterial* strains assessed using AATCC – 147 and AATCC – 100 procedures. The shaker bath experiment is performed to assess the durability of the Ag NS/PCL coated cotton fabric and elucidated that after 8 h of durability test. The durability of the surface-modified fabric is assessed using 8 h of shaker bath experiments; the modified fabric exhibits antibacterial activity comparable to that of the unwashed fabrics and exhibits reasonable adherence of Ag NS with the fabric. From the obtained results, Ag NS/PCL-modified cotton fabric exhibits excellent antibacterial activity against both gram-positive and gram-negative strains with durability.

Keywords: silver nanoparticles; green synthesis; polycaprolactone; antibacterial activity; cotton fabric; dip-coating.

1. Introduction

Amongst the various types of fabrics used in our day-to-day wearable textiles like daily wear, child wear, sportswear, health care, etc., cotton fabric is most commonly used for their fabrication. The cotton fabric is more versatile owing to its most beneficial properties such as good air permeation, water absorption, comfort to wear, etc. The cotton fabric possesses a high wetting ability leading to the adherence of sweat, spills, etc., leading to the drawback of bacterial growth [1-3]. Cotton fabrics are widely used in the healthcare sector to manufacture textiles such as patient gowns, beds, bandages, healthcare worker uniforms, etc. These healthcare textiles can easily get contaminated by bacterial strains through body fluids such as urine, pus, blood, etc., during patient care activities causing severe threats of spreading infections to visitors/other patients [4,5].

Further, domestic washing cannot permanently remove bacterial growth from the fabrics owing to the resistance developed by the bacteria; therefore, the addition of antibiotics is also not feasible [6,7]. In this regard, the focus has shifted towards nanotechnology, where numerous reports demonstrated that loading suitable nanoparticles (NPs) on the fabric incorporates several properties like self-cleaning, flame retardancy, antibacterial activity, UV protection, etc. [8-10]. In this regard, metal and metal oxide-based NPs are most widely used to impart antibacterial activity to fabrics. Since metal and metal oxide-based NPs are proven to generate more reactive oxygen species (ROS), they can effectively decline bacterial biofilm formation. It is also reported that the NPs are found to show activity against multi-drug resistance (MDR) microbes due to the generation of ROS [11,12]. Therefore, NPs incorporated fabrics are suitable and effectively help to mitigate MDR bacterial strains [13,14].

Metal NPs are found to have inherent antibacterial activity owing to their metal ion-releasing phenomenon. Especially silver (Ag) NPs has gained attention from global researchers all over the world as they possess efficient natural disinfectant property [15,16]. Ag NPs are found to show more toxicity towards bacterial strains because of their metal ion release kinetics [17], where the ions can easily bind with the cell membrane by electrostatic interaction and disrupt cellular functions [18,19]. The Ag NPs can be prepared in size ranging from a few nanometers to tens of nanometers and, therefore, can be easily uptaken by the bacterial cell due to its sub-micron size, and interacts with proteins and DNA, resulting in bactericidal effects [20]. Therefore, exploring the properties of Ag NPs with respect to size, shape, reaction kinetics, etc., will greatly promote the advancement of nanoscience towards technologies. There are numerous techniques for the preparation of Ag NPs, such as chemical reduction of silver precursor, electrochemical method, sonochemical method, etc. [21]. In most cases, the preparation involves toxic chemicals leading to adverse effects and toxicity. Thus, it brings a concern about how to use them in close proximity to humans with minimal toxicity [22]. In these aspects, scientists have developed bio-reduction techniques as an alternative to chemical techniques [23,24]. In bio-reduction techniques, biologically active compounds synthesized from natural products like plant extract are used, which helps in the reduction of metallic ions to its NPs. Numerous reports dealt with the conjugation of Ag NPs to the cotton fabrics through dip coating, in-situ, pad-dry-cure, hydrothermal methods, etc. Ahmed *et al*. [25] prepared Ag NPs through a bio-synthesis route using *Streptomyces laurentii* R-1 strain. Further, the Ag NPs were embedded over cotton fabrics employing the pad-dry-cure method. The modified cotton fabric was able to inhibit *B. subtilis*, *P. aeruginosa*, and *E. coli* bacterial strains with the zone of inhibition (ZOI) of 2.63 mm, 1.23 mm, and 1.91 mm, respectively. However, the team reported that with consecutive washes, the fabric loses its bactericidal activity. Shaheen *et al*. [26] modified the surface of cotton fabrics using Ag NPs isolated through an in-situ route by reducing Ag^+ ions with different fungal strains. The ZOI studies of Ag NPs coated fabric shows display antibacterial activity against *S. aureus* and *E. coli* with ZOI of 26 mm and 22 mm zone against *S. aureus* and *E. coli*, respectively, substantiating its antibacterial activity. The team reported that there is a decrease in antibacterial activity after washing cycles.

From the above literature data, it is understandable that Ag NPs embedding over the fabrics using different techniques can impart excellent antibacterial activity to the fabrics. Even though the fabric developed using such techniques possess higher antibacterial activity, However, in real-time applications, under harsh conditions like washing, aberration, etc., degrade the quality of the coatings gets degraded. In those conditions, the NPs coated over the fabric will be detached easily, resulting in reduced activity of the modified fabric. In this

context, numerous kinds of many literature reports dealt with the use of polymers as binders for the Ag NPs to hold better on the cotton fabric of highly durable coatings of NPs [27,28], whereas scientists use polymers as the binder for the Ag NPs to hold it better on the cotton fabric. Zhu *et al*. [29] developed an antibacterial cotton fabric by embedding Ag NPs prepared by the extract of honeysuckle through the crosslinker, i.e., poly maleic acid and citric acid. Even after 50 washing cycles, the modified cotton fabric displayed 99% bactericidal efficiency against *E. coli* and *S. aureus* assessed through the colony counting technique. Gao *et al*. [30] developed the antibacterial cotton fabric by embedding Ag NPs coated cotton fabric with the help of polydopamine, which was again treated with polydimethylsiloxane to enable super-hydrophobicity. The ZOI studies revealed that the modified fabric displays antibacterial activity against *E. coli* and *S. aureus* strains with adequate washing durability. Similarly, various literature states that the adherence of Ag NPs over the cotton fabric is improved by the addition of polymer binders. However, most of the polymers are either water soluble, non-degradable, or toxic to human cell lines, which hinders their real-time usage.

Polycaprolactone (PCL) is a biodegradable and food and drug administration-approved polyester polymer that is extensively used for biomaterial fabrication. However, the use of PCL as a binder for the Ag NPs to be coated over cotton fabric is not yet explored. As PCL is a biodegradable, non-toxic polymer that is hydrophobic, it can hinder the interaction of polar solvents with the fabric to a certain extent. In this aspect, in the present work, aqueous green synthesized silver nanospheres (Ag NS) are coated over cotton fabric through a simple dip-coating route. Further, for adherence, Ag NS-coated cotton fabric is immersed in the PCL/chloroform solution. The modified fabrics are assessed for antibacterial activity and durability after shaker bath experiments.

2. Materials and Methods

2.1. Materials required.

Silver nitrate (>99% pure), nutrient broth, and nutrient agar are obtained from Sigma Aldrich, India. The leaves of *Maranta arundinaceae* are collected from the herbal garden Chettinad Academy of Research and Education (CARE). 100% pure cotton fabric is purchased from the local market.

2.2. Preparation of leaf extract.

Fresh leaves of *Maranta arundinaceae* are collected, thoroughly cleaned using milli-Q water, and sliced into small pieces of size ~0.5 cm × 0.5 cm. 1.7 g of sliced leaves are suspended in 100 ml milli-Q water, and the mixture is allowed to boil at 100°C for 15 min. The filtrate is collected through filtration and stored in an airtight container for the preparation of Ag NS.

2.3. Preparation of Ag NS.

The obtained leaf extract is used as a bio-reducing and capping agent for the preparation of Ag NS. 0.1 mM of silver nitrate is dissolved in a beaker containing 100 ml of distilled water. To the above solution, 10 ml of the prepared leaf extract is added in a drop-wise manner under continuous stirring. The mixture is constantly stirred at 100 rpm for 15 min at 60°C. Over time, the color of the solution turns yellowish brown, indicating the formation of Ag NS.

2.4. Antibacterial activity of Ag NS suspension.

In the present study, the Ag NS is prepared by the green synthesis route via leaf extract of *Maranta arundinaceae*. It has been reported that the antibacterial activity of NPs depends on the size, shape, and precursor used. Therefore, the bactericidal activity of Ag NS prepared through the green synthesis route is evaluated through UV-Vis spectroscopic analysis and well diffusion technique. *Escherichia coli (E. coli), Staphylococcus epidermidis (S. epidermidis),* and *Methicillin-Resistant Staphylococcus aureus (MRSA) strains* are selected to analyze the antibacterial activity.

2.4.1. UV-Vis spectroscopic analysis.

Different quantities of Ag NS suspension (50 µl, 25 µl, 12.0 µl, 6.0 µl, and 3.0 µl) are added to 5 ml nutrient broth in sterile test tubes. Then, test tubes are suspended with 50 µL of selected bacterial strains and are incubated at 37°C for 24 h. The incubated samples' optical density (OD) is then recorded using a UV-Vis spectrometer Shimadzu, Japan, at 600 nm and compared with the control. The samples with high absorbance indicate high bacterial growth, while the reduction in absorbance validates the bactericidal activity of Ag NS.

2.4.2. Well diffusion method.

The selected bacterial strains are cultured and incubated in nutrient broth (50 ml) at 37°C for 24 h. The incubated strains are uniformly spread over the sterilized nutrient agar plates by the lawn culture method. Different quantities of Ag NS suspension (200 µl, 150 µl, 100 µl, 75 µl, 50 µl, 25 µl, 12.0 µl, 6.0 µl, and 3.0 µl) are loaded on the wells developed on the plates and incubated for 24 h at 37°C. The obtained ZOI values are noted and compared.

2.5. Fabrication of Ag NS/PCL modified cotton fabric.

At first, Ag NS is embedded over the fabric surface by a simple dip-coating method. Then, the cotton fabric purchased is thoroughly washed thrice with distilled water followed by ethanol, air dried, and used for further studies. The cotton pieces of the required dimension are immersed in the prepared Ag NS solution (preparation detailed in section 2.3) for 1 h. After the stipulated time, the cotton pieces are removed and air-dried. The dried Ag NS-modified fabric is collected in an airtight container and is subjected to various biological studies. Further, dried Ag NS treated fabric is immersed in the polymer solution containing 0.05 g of polycaprolactone (PCL) dissolved in 10 ml of chloroform for 10 min and dried in air to obtain Ag NS/PCL modified fabric.

2.6. Antibacterial activity of Ag NS and Ag NS/PCL modified fabrics.

The antibacterial activities of the Ag NS and Ag NS/PCL modified cotton fabrics are assessed using the American Association of Textile Chemists and Colorists (AATCC) 147-2004 and AATCC 100-2004 standards against *E. coli, S. epidermidis,* and *MRSA.*

2.6.1. AATCC-100 technique.

The untreated, Ag NS treated, and Ag NS/PCL treated cotton fabrics are cut into circular shapes with a diameter of 4.8 cm. 10 ml of inoculum is prepared by inoculating the bacterial strains into the fresh nutrient broth and incubated for 24 h at 37°C. Then the bacterial

concentration is adjusted to 10^5 CFU/ml. 10 ml of diluted inoculum is added into each well of 6 well plates containing the test fabrics. Then the samples are incubated for 24 h at 37 °C. After 24 h, the sample mediums are serially diluted with nutrient broth, a known quantity of the inoculum is spread uniformly over agar plates, incubated at 37°C, and the colonies are counted [4]. The percentage reduction of bacteria after the formula calculates 24 h incubation,

$$\%R = \frac{A - B}{A} \times 100$$

where R is the reduction in colony count, A is the no. of colonies formed by treating the uncoated specimen, and B is the no. of colonies formed by treating coated specimen.

2.6.2. AATCC-147 method.

Pristine and modified cotton fabrics are cut into rectangular swatches of size 2.5 cm × 5 cm and sterilized. A loopful of bacterial culture is taken, and five parallel streaks are made over the agar plate, where the pristine and modified cotton fabrics are placed transversely to the culture streak direction and incubated at 37°C for 24 h. The size of the clear zone is evaluated by the formula,

$$W = \frac{T - D}{2}$$

where W is the width of the clear zone, T is the total width of the test specimen with zone, and D is the width of the test specimen [31,32].

2.7. Durability of modified fabrics.

The durability of Ag NS and Ag NS/PCL modified fabrics are assessed by the shaker bath experiment. Modified fabrics are immersed in a beaker containing distilled water, kept it in a shaker bath for 8 h at room temperature to depict the real-time washing procedure, and air dried. The dried washed fabrics are subjected to antibacterial activity following the same procedure described in section 2.6.

2.8. Characterization techniques.

The morphology of the prepared Ag NS is analyzed by employing the scanning electron microscope (SEM) [JEOL JSM 7001F, Japan] and Transmission Electron Microscope (TEM) [JEOL-2100, Japan]. The elemental compositions of the prepared samples are assessed by the energy dispersive X-ray spectroscopy (EDX) which is attached to SEM. The crystal structure of Ag NS is assessed by X-ray Diffraction (XRD) pattern obtained using Panalytical X'Pert Powder X'Celerator Diffractometer. The functional groups present in the plant extract and Ag NS suspension are estimated from the Fourier Transform Infrared (FTIR) spectra recorded with Bruker optics, Alpha model, Germany. The formation of Ag NS is confirmed from the UV-Vis absorption spectra recorded in the range 300 nm to 700 nm using UV–Vis Spectrometer, Perkin Elmer, Lambda 25, USA. X-ray photoelectron spectroscopic (XPS) [Shimadzu ESCA 3100] analysis is performed to estimate the chemical states of elements present in the prepared Ag NS sample. The surface morphologies of Ag NS and Ag NS/PCL modified cotton fabric are visualized through SEM images recorded using SU1510, Hitachi, Japan, and FEI Quanta FEG 200, USA. The EDX spectra of Ag NS and Ag NS/PCL-modified cotton fabrics display the presence of Ag moiety in the modified fabric.

3. Results and Discussion

3.1. Characterization of Ag NS.

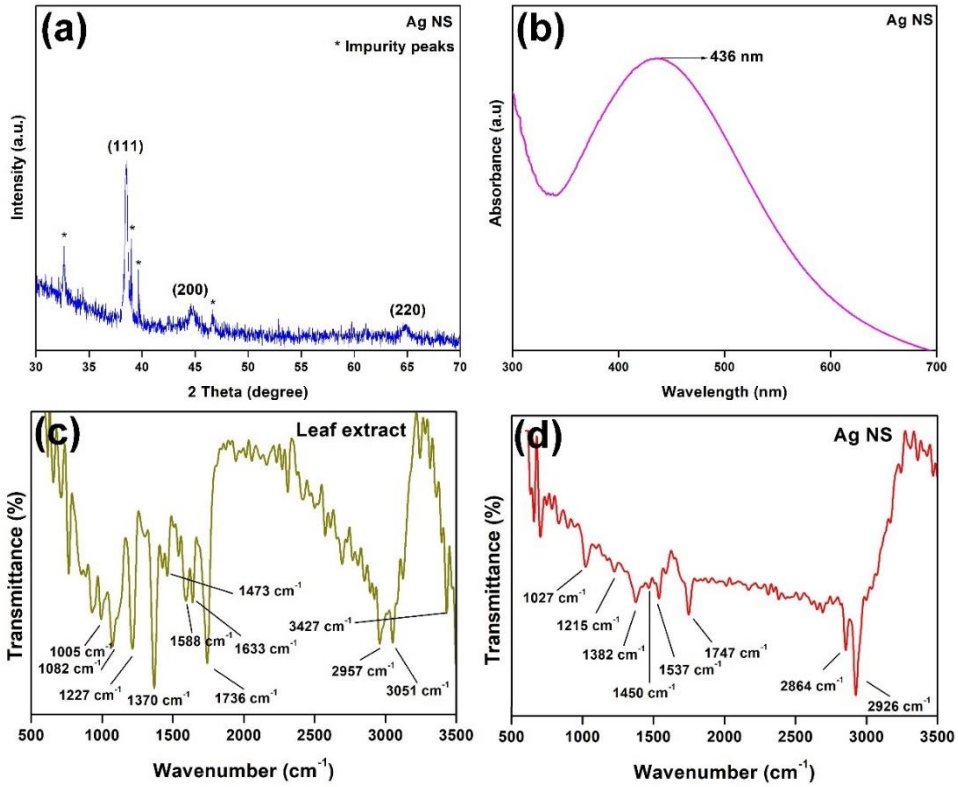

Figure 1. (a) XRD of Ag NS, **(b)** UV-Vis spectrum of Ag NS suspension, FTIR of **(c)** leaf extract, and **(d)** Ag NS suspension.

X-ray diffraction (XRD) pattern displays diffraction peaks that validate the crystalline nature of Ag NS synthesized by green synthesis route using an aqueous extract of Maranta arundinaceae leaves (Figure 1a). The diffraction peaks of Ag NS are obtained at 2θ = 38.5°, 44.8°, and 64.9° attributed to the miller indices (111), (200), and (220), respectively which are well matched with JCPDS File no. 03-065-2871 [33,34]. Therefore, it confirms that the Ag^+ ions are reduced by bioactive compounds present in the *Maranta arundinaceae* leaf extract to obtain a well-defined crystalline Ag NS [35,36]. However, there are other peaks that originated from the impurities (bio-molecules). Apart from the diffraction peaks corresponding to Ag crystal, impurity peaks can be seen. These impurity peaks originated from the AgCl and $AgNO_3$ crystals. During the preparation of Ag NS, a lower degree of Ag^+ ions react with the Cl^- from the phytochemicals to form inorganic AgCl. Similar results are reported where this phenomenon is common in the green synthesis route [37]. Further, during sample preparation of Ag NS for XRD analysis, the Ag NS suspension is drop cast over the suitable substrate, and diffraction peaks are analyzed. Therefore, unreacted Ag^+ and NO_3^- ions are introduced into the sample and form $AgNO_3$ crystals, forming impurity peaks. The UV-visible spectroscopic analysis validates the presence of Ag NS in the prepared suspension where the characteristic λmax peak appears at 436 nm (Figure 1b). Further, the FTIR analysis is performed for aqueous leaf extract (Figure 1c) and Ag NS suspension (Figure 1d). The peak values are summarized in Table 1. From the FTIR spectra, it shows that the peak intensities (ratio) present in the Ag NS suspension declined when compared to the leaf extract, and hence, it is clear that the phytochemicals present in the leaf extract take part in the reduction of Ag^+ to Ag^0. Especially,

the peaks corresponding to phenolic compounds and proteins are very much diminished owing to the interaction of Ag moiety with the hydroxyl groups of phenol and amine groups of proteins responsible for forming the capping phenomenon [38,39].

Table 1. Peak values from FTIR spectra

Sl. No.	Wavenumber (cm^{-1})		Functional group	Vibration	Ref
	Leaf extract	Ag NS			
1	3427	-	-OH group of phenolic compounds	Stretching	[40]
2	3051	2925	$-CH_3$ group	Asymmetric stretching	[40]
3	2957	2864	C-H group of alkanes or secondary amine	Stretching	[40]
4	1736	1747	C-C group (non-conjugated)	Stretching	
5	1633 & 1588	1537	-C=C- present in flavonoids and terpenoids, and carbonyl group (-C=O)- of proteins or amide I	Stretching	[38] [40]
6	1473	1450	N-H group of proteins	Stretching	[39] [40]
7	1370	1382	N=O of nitro compound		[39]
8	1227	1215	C-N of amines	Stretching	[39]
9	1082	1027	C-N (amines of proteins)	Stretching	[39]

The chemical states of Ag and the capping agent present in the Ag NS are evaluated by recording the XPS data shown in Figure 2a-c. From the de-convoluted spectra for Ag (3d), the chemical states such as Ag $3d_{3/2}$ and Ag $3d_{5/2}$ are found at binding energies of 368 eV and 374 eV, respectively which are in good agreement with the literature data [41]. Also, an extra peak at binding energy 370 eV is attributed to the interaction of oxygen from the biomolecules to the Ag moiety [42]. The C 1s peak is de-convoluted into three peaks Figure 2b at binding energies 284 eV, 285 eV, and 288 eV attributed to the C=C of hydrocarbon, carbon in C-O, and from the carbonyl group C=O, respectively [43]. The chemical state of O found in the capping biomolecule is evaluated in Figure 2c, displaying a peak with the binding energy of 532 eV originating from O 1s of the carbonyl group.

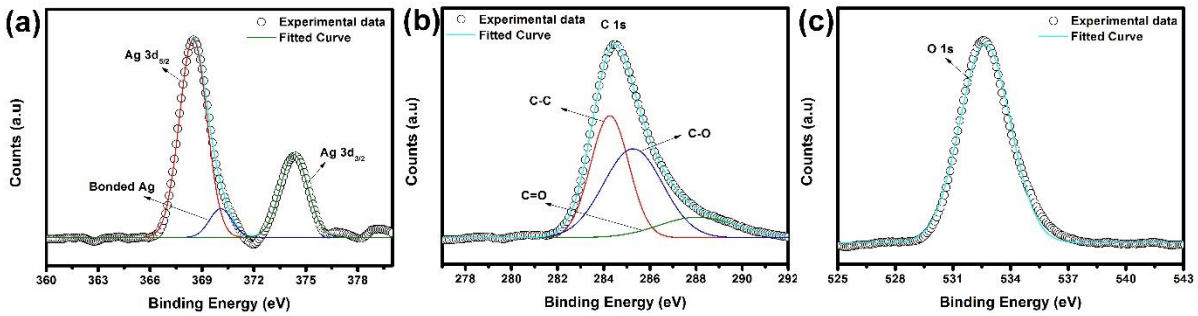

Figure 2. XPS analysis of Ag NS displaying de-convoluted peaks corresponding to **(a)** Ag 3d, **(b)** C 1s, and **(c)** O 1s.

The morphology and elemental analysis of Ag NS are assessed by the SEM images (Figure 3a) and EDX spectra (Figure 3b), respectively. The SEM images of Ag NS display near spherical-shaped structures in the nano regime [44]. The Ag NS are found distinct with mono-dispersed nature having a size ranging in ~20 nm scale. The residual leaf extract over the surface of Ag NS is not visualized through SEM images. However, the Ag NS are found with a certain degree of aggregation that may be facilitated by the presence of biological components while air drying for sample analysis. The leaf constituents present in the sample can be validated through EDX analysis (Figure 3b). The appearance of O and C in the EDX spectra originated from the biomolecules that bind to the Ag NS as the capping agent can be seen. Along with them, the peaks attributed to the Ag Lα and Ag Lβ are found at 3 eV and 3.1 eV,

respectively. Also, a high-intensity peak attribute to Al Kα originated from the Al substrate in which the samples are held.

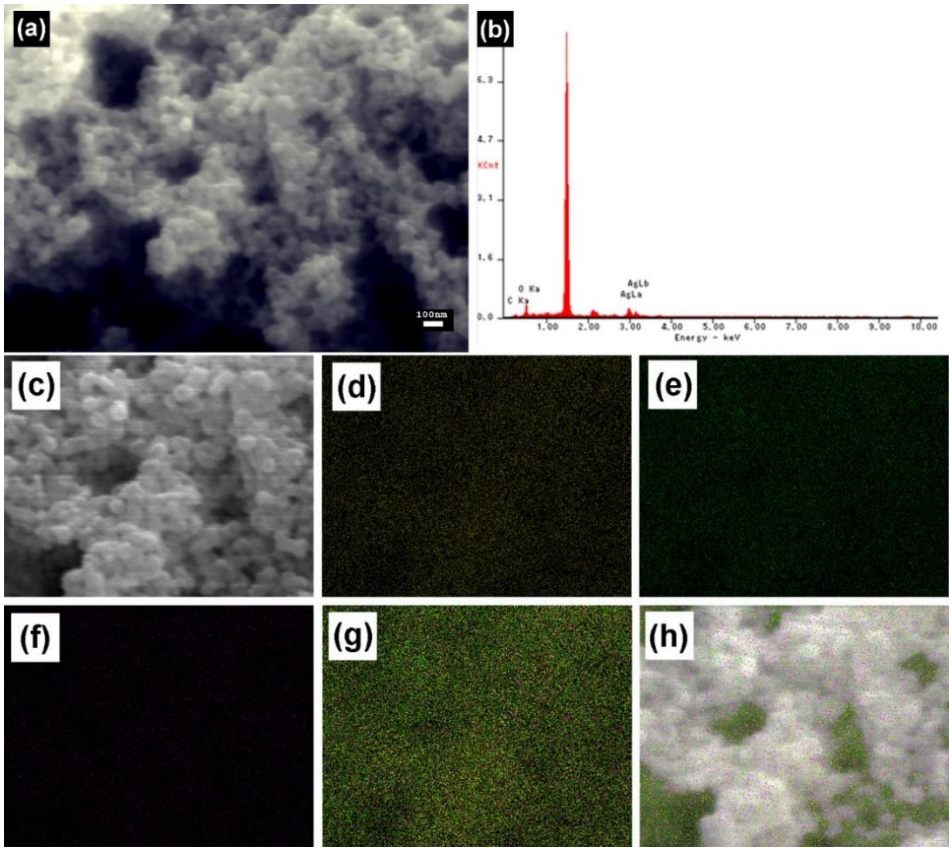

Figure 3. (a) SEM image and **(b)** EDX spectrum of Ag NS; EDX mapping images **(c)** recorded SEM image region, **(d)** Ag, **(e)** O, **(f)** C, **(g)** overall mapping spectra and **(h)** overall mapping spectra along with corresponding SEM image.

Also, the peak that appeared at ~2.1 eV corresponds to the peak of Au, which is sputter coated during sample preparation to enhance the output image. Further, to elucidate the formation of Ag NS, EDX mapping analysis is carried out [Figure 3c-h]. The mapping spectra show the presence of Ag attributed to the X-ray originating from the L shell of Ag NS (Figure 3d). Likewise, the presence of O and C are contributed by the biomolecules of plant extract that bind to the Ag moiety (Figure 3e&f).

Since the capping agent is not seen in the SEM images, TEM analysis is carried out. The TEM images of the Ag NS at different magnifications are shown in Figure 4a-c. The TEM images of Ag NS display spherical-shaped structures with a high degree of symmetry (Figures 4a&b). The figure shows that Ag NS are nearly mono-dispersed and are capped with a thin layer of biological components from leaf extract (Figure 4c). The thickness of the phytochemical constituents that are capped over the Ag NS is found to be ~2 nm. The particle size of Ag NS is found to be less than 20 nm which is in agreement with the SEM images. The capping agent restricts the growth of Ag NS, leading to small-sized particles (< 20 nm), and provides symmetric growth of Ag nuclei leading to nanospheres while crystal growth [45].

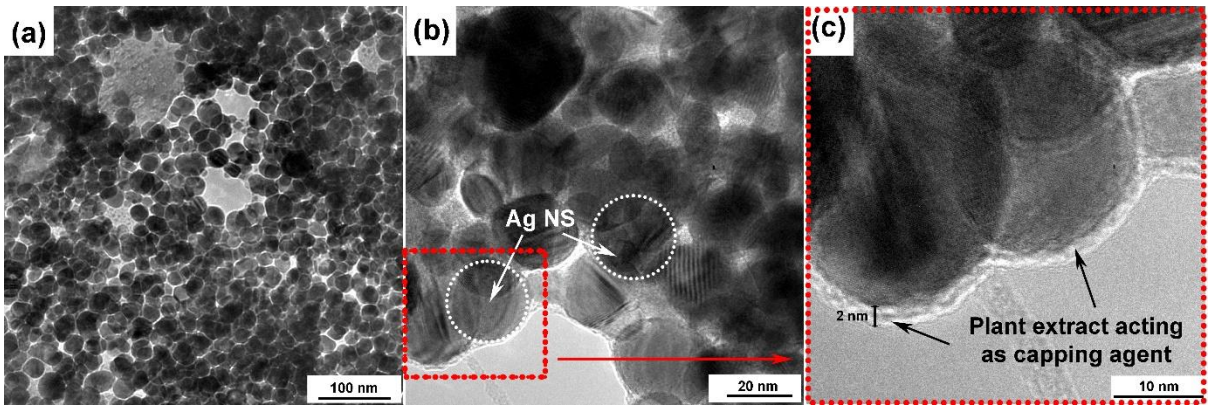

Figure 4. TEM images of Ag NS at different magnifications.

3.2. Antibacterial activity of Ag NS suspension.

The bactericidal effect of silver has been well-known for many decades and employed in many bio-medical applications [46]. In the present study, the use of Ag NS for the fabrication of hygienic fabric has been implemented. Here, Ag NS prepared via the biosynthesis method is used as an antibacterial moiety to be embedded in cotton fabric. Therefore, it is necessary to evaluate the antibacterial activity of Ag NS before coating it over the fabric. The UV-vis spectroscopic analysis and well diffusion technique are employed to elucidate the bactericidal activity of Ag NS against *E. coli*, *S. epidermidis*, and *MRSA* bacterial strains as per the procedures given in section 2.4. From the obtained OD values [Table 2], there is a considerable reduction in the values of *E. coli* culture when 6 µl of Ag NS is added. Likewise, a significant reduction is seen for *S. epidermidis* and *MRSA* when 25 µl of Ag NS is added, substantiating the minimum inhibitory quantity. Similarly, the well diffusion technique revealed that with 6 µl Ag NS suspension, well-defined ZOI is formed for all the bacterial strains. However, the zone diameter is higher against *E. coli* (10 mm) than *S. epidermidis* (8 mm) and *MRSA* (8 mm) bacteria. As the Ag NS suspension quantity increased, the ZOI diameter improved against all the bacterial strains (Table 2) (Supplementary Information, Figure S1). These results show that the prepared Ag NS possesses antibacterial activity against both gram-positive and gram-negative bacterial strains.

Table 2. Optical density and ZOI values of bacterial culture after incubating with different quantities of Ag NS suspension.

Sl. No.	Sample quantity (µl)	Absorption (a.u.)			Zone of Inhibition (cm)		
		E. coli	*S. epidermidis*	*MRSA*	*E. coli*	*S. epidermidis*	*MRSA*
1	50	0.02 ± 0.002	0.013 ± 0.00	0.013 ± 0.002	1.4	1.1	1.1
2	25	0.01 ± 0.002	0.098 ± 0.00	0.006 ± 0.001	1.3	1.1	1.1
3	12	0.01 ± 0	0.582 ± 0.05	0.137 ± 0.019	1.2	1.0	0.9
4	6	0.01 ± 0.002	0.591 ± 0.02	0.791 ± 0.01	1.0	0.8	0.8
5	3	0.51 ± 0	0.577 ± 0.05	0.841 ± 0.071	-	-	-
6	Control	0.64 ± 0.07	0.768 ± 0.05	0.945 ± 0.01	1.8	1.3	-

3.3. Characterization of Ag NS/PCL coated cotton fabric.

FTIR spectra of the uncoated, Ag NS coated, and Ag NS/PCL coated cotton fabrics are provided as supplementary information in Figure S2. The positions of bands in the pristine and modified fabrics are summarized in Table 3. From Figure S2 and tabulated data, it is clear that the characteristic peaks of the cotton are obtained for all the specimens, i.e., coated and uncoated fabrics. Also, it is inferred that the peak positions are not significantly changed when Ag NS or Ag NS/PCL is immobilized over the fabric. Further, new peaks with respect to Ag

NS and Ag NS/PCL coating are not inferred through FTIR spectra as their elemental composition is very low compared to bulk cotton fabric.

Table 3. Peak values from FTIR spectra of coated and uncoated fabrics.

Sl. No.	Wavenumber (cm^{-1})			Functional group	Vibration	Ref
	Cotton	Ag NS-coated cotton	Ag NS/PCL coated cotton			
1	3339	3331	3340	-OH groups of cellulose, lignin, and water	Stretching	[47,48]
2	2889	2898	2889	C-H present in cellulose and hemicellulose	Asymmetric stretching	[47,48]
3	1630	1630	1632	-OH groups from water molecules	Bending	[48]
4	1420	1420	1428	C-H from the methylene group	Wagging	[48]
5	1322	1322	1322	C-H from the methylene group	Bending	[48]
6	1027	1029	1027	C-O of the polysaccharide in cellulose	Stretching	[47,48]
7	668	668	668	Anhydro-glucopyranose in B-glycosidic ring of cellulose	Wagging	[48]
8	551	551	545	Anhydro-glucopyranose in B-glycosidic ring of cellulose	Twisting	[48]

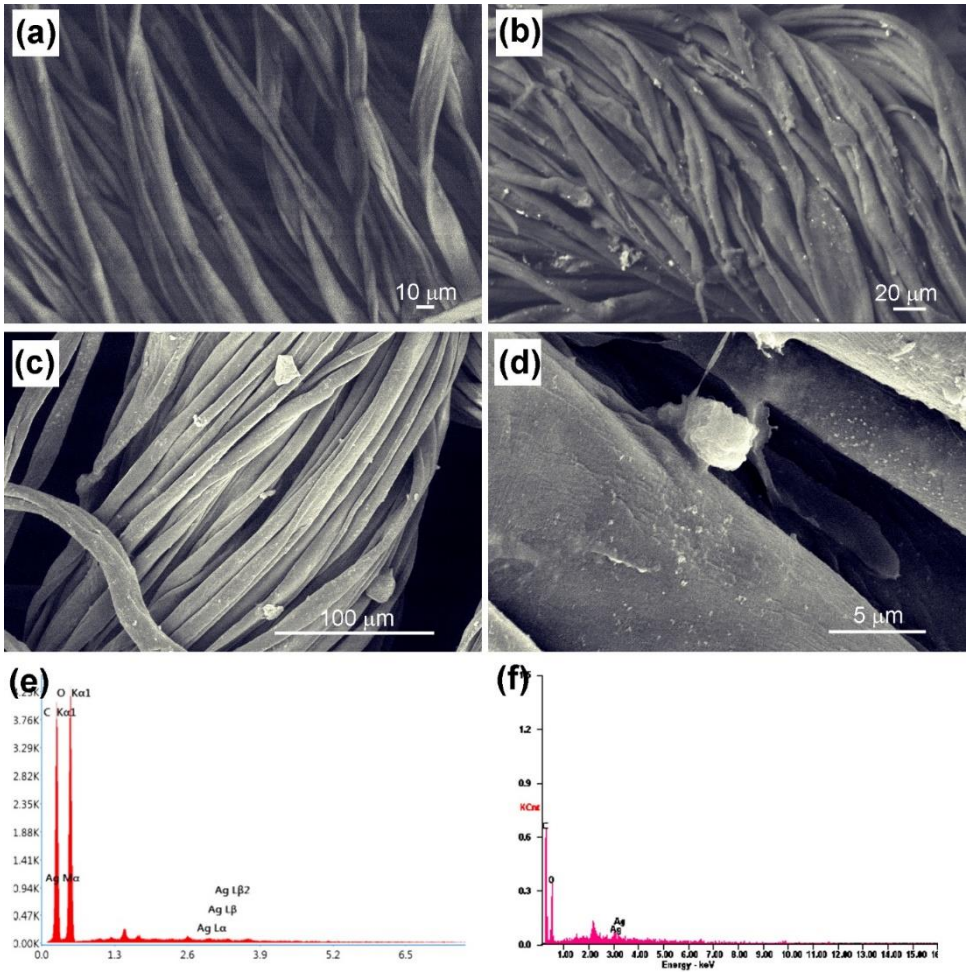

Figure 5. SEM image of **(a)** untreated, **(b)** Ag NS treated, **(c)** Ag NS/PCL treated, and **(d)** magnified image of Ag NS/PCL treated cotton fabric. EDX spectra of **(e)** Ag NS treated and **(f)** Ag NS/PCL treated cotton fabric.

SEM images and EDX spectra of pristine, Ag NS modified, and Ag NS/PCL modified cotton fabrics are shown in Figure 5a-f. In Figure 5a, the surface morphology of pristine cotton fabric shows a clean surface, whereas in Ag NS modified cotton fabrics, the deposition of Ag NS on the surface of fabrics can be seen (Figure 5b). Likewise, in the case of Ag NS/PCL modified fabrics, the Ag NS can be found embedded over the fabrics (Figure 5c). The

magnified SEM image shown in Figure 5d substantiates that the Ag NS is not detached from the fabric while coating with PCL and also has a uniform distribution. The EDX spectra (Figure 5e&f) show that Ag moiety is present over the modified fabrics [49].

3.4. Antibacterial activity of Ag NS/PCL coated fabric.

3.4.1. AATCC-100 method.

The antibacterial activity of Ag NS and Ag NS/PCL modified fabric is quantitatively assessed by the AATCC-100 method as per the methodology given in section 2.6.1. The modified and control fabrics are inoculated along with nutrient broth containing bacterial strains, which are then incubated at 37°C for 24 h, subsequently, their OD values are recorded at 600 nm and are tabulated in Table 4. The OD values of inoculum treated with modified fabrics are found to be reduced compared to the control inoculum. From the OD values, the inhibition efficiencies (%) are calculated and listed in Table 4. The inhibition efficiency (%) of Ag NS treated cotton fabrics is >96% against *E. coli, S. epidermidis*, and *MRSA*. Likewise, Ag NS/PCL treated cotton fabrics display inhibition efficiencies of >95% against all the selected bacterial strains. The inhibition efficiency (%) is found to be more or less similar in the case of Ag NS and Ag NS/PCL-modified cotton fabrics.

Table 4. OD values and reduction efficiencies of Ag NS and Ag NS/PCL modified fabrics against *E. coli, S. epidermidis*, and *MRSA*.

Sl. No.	Parameters	*E. Coli*		*S. epidermidis*		*MRSA*	
		OD value	Reduction efficiency (%)	OD value	Reduction efficiency (%)	OD value	Reduction efficiency (%)
1	Untreated cotton fabrics	0.8	-	0.9	-	0.85	-
2	Ag NS-treated cotton fabrics	0.031	96.13	0.034	96.22	0.032	96.24
3	Ag NS/PCL treated cotton fabrics	0.033	95.9	0.033	96.33	0.029	96.59

Further, the inoculated cultures are spread on the sterile agar plates separately and incubated at 37°C for 24 h. Then the bacterial colonies from each plate are counted, and the reduction rate (%) is calculated. The plates cultured from the inoculum treated with Ag NS and Ag NS/PCL modified fabrics display zero colony growth [supplementary information; Figure S3] against *E. coli, S. epidermidis*, and *MRSA* substantiating a 100% reduction rate.

3.4.2. AATCC-147 method.

Further, the antibacterial activity of uncoated Ag NS and Ag NS/PCL modified cotton fabrics are assessed by the AATCC-147 method against the same bacterial strains. The ZOIs formed around the fabrics are shown in Figure 6a-i. Figure 6a-c depicted that the control fabric has no bactericidal activity against the selected bacterial strains where no zones are seen. Also, bacterial growth is found along the direction of the streak, even in the vicinity of fabrics (marked by black arrows). However, the ZOIs are clearly observed in the case of Ag NS-modified cotton fabrics (Figure 6d-f), where gram-negative strain is inhibited effectively compared to gram-positive strains. Also, it is to be noted that when PCL is overcoated on Ag NS-modified fabric, the ZOIs tend to decrease for all the bacterial strains (Figure 6g-i). The obtained ZOI values are summarized in Table 5, from which the ZOI for *E. coli* is found to be two-fold high for Ag NS when compared to Ag NS/PCL. Similarly, for *S. epidermidis* and *MRSA*, the ZOIs are higher in the case of Ag NS than Ag NS/PCL. This reduction in the ZOI

size is due to the restriction of the Ag^+ release by the PCL polymer that acts as both a binder and capping agent.

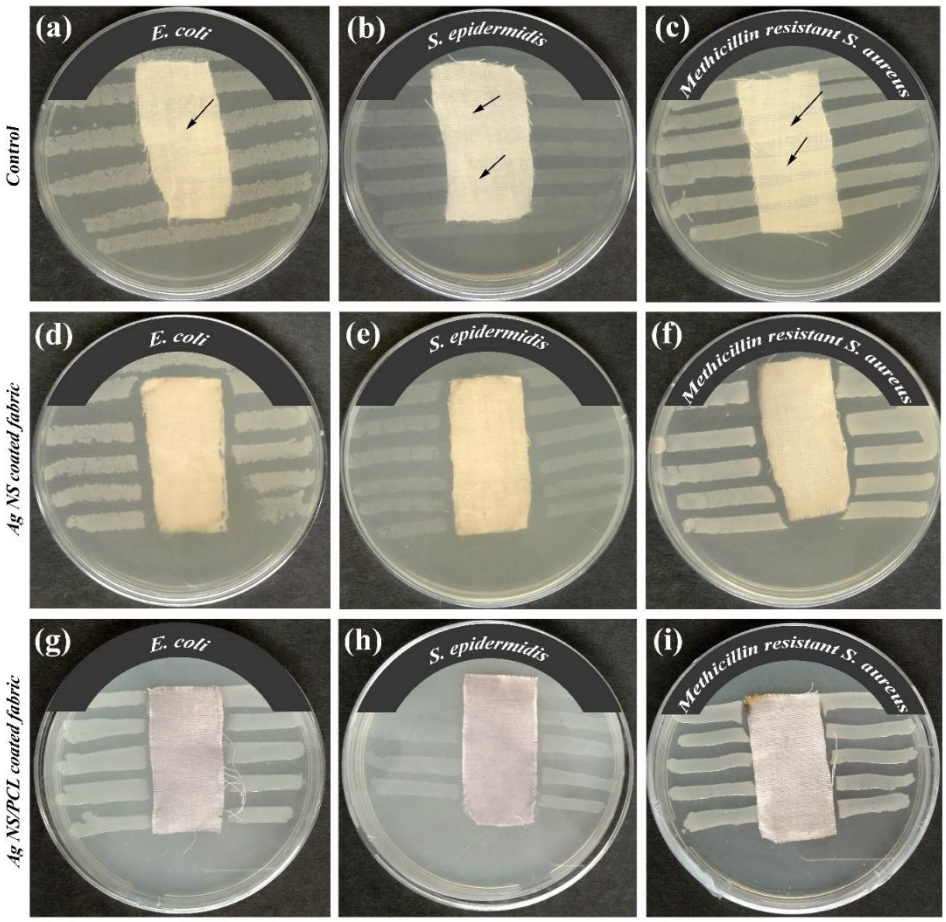

Figure 6. Antibacterial activity of **(a-c)** control, **(d-f)** Ag NS, and **(g-i)** Ag NS/PCL modified cotton fabrics against *E. coli*, *S. epidermidis*, and *MRSA*.

Table 5. Width of clear zone extracted through AATCC-147 method.

Ag NS modified fabrics (cm)									**Ag NS/PCL modified fabrics (cm)**								
E. coli			***S. epidermidis***			***MRSA***			***E. coli***			***S. epidermidis***			***MRSA***		
T	**D**	**W**	**T**	**D**	**W**	**T**	**D**	**W**	**T**	**D**	**W**	**T**	**D**	**W**	**T**	**D**	**W**
3.5	2.5	0.5	3.2	2.5	0.35	3	2.5	0.25	3	2.5	0.25	3	2.5	0.25	2.9	2.5	0.2

3.5. Durability.

The durability of Ag NS and Ag NS/PCL modified fabrics are assessed by performing the antibacterial activity using the AATCC-147 method after 8 h shaker wash. The results are shown in Figure 7a-f. Figure 7a-c shows that the ZOIs are reduced in the Ag NS-modified fabric for all the bacterial strains (W = ~0 cm). Further, in the case of *S. epidermidis*, Ag NS-coated fabric shows a significant growth of bacterial cells without zone formation under the fabrics (W = ~0.1 cm). But no bacterial growth is found below the fabrics, substantiating that a low degree of Ag moiety is present. However, in the case of especially against *MRSA* strain, the bacterial cells tend to grow below the fabric, validating the instability of the Ag NS coated fabric against drug resistance strain after the washing process [inset of Figure 7c] (W= ~0.1 cm). This is owing to the fact that the Ag NS is detached from the fabric during washing cycles, as there is no binder involved.

In contrast, Ag NS/PCL modified fabrics are found to be stable after the durability studies displaying almost the same clear zone (W=0.3 cm, 0.15 cm, and 0.2 cm against *E. coli*,

S. epidermidis, and *MRSA* strains) as that of the unwashed fabrics. Even though there is a decline in activity, especially for *S. epidermidis*, compared to Ag NS coated fabric, the PCL provides substantial support for the Ag NS to anchor over the fabrics. Here, the Ag NS/PCL modified fabrics also display better activity against *E. coli* than *S. epidermidis* and *MRSA* strains. This proved that the PCL acts as a binder that declines the Ag NS detachment while washing cycles and as a capping agent that helps in the sustained release of Ag^+ ions.

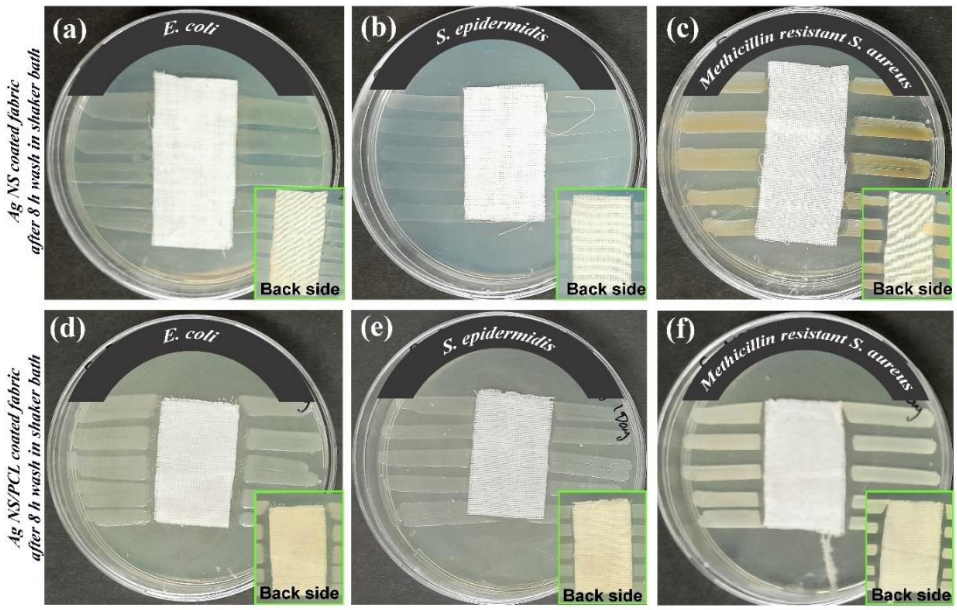

Figure 7. Durability studies assessed using 8 h wash in a shaker bath.

3.6. Possible antibacterial mechanisms of Ag NS/PCL modified fabric.

Ag NPs are significantly known for their effective antibacterial activity owing to their multiple synergistic routes of bactericidal effect. The penetrative nature of Ag NPs within the bacterial cell wall subsequently results in structural damage of membranes leading to bactericidal activity. However, in the present case, the Ag NS is embedded over the fabrics, and therefore, the NPs penetration may not be the absolute cause of antibacterial activity. But, the release of Ag^+ ions from the surface of NPs is one of the primary mechanisms behind the bactericidal activity. The Ag^+ ions can be readily dissociated from the Ag NS attached to the fabrics. Also, while adding PCL, the activity reduces owing to the restriction of Ag^+ ions released by the polymer, which substantiates the fact that the Ag^+ ions are responsible for the antibacterial activity of Ag NS against *E. coli*, *S. epidermidis*, and *MRSA*. The Ag^+ ions released from the Ag NS take part in ROS reactions which disrupts the cell wall of bacteria. Further, internalized Ag^+ ions interact with intra-cellular enzymes causing ribosomal destabilization and resulting in the lower protein expression ceasing further multiplication. Ag^+ ions also interact with DNA bases and damage the backbone of DNA, resulting in bacteriostatic activity and stopping the further multiplication of bacteria.

4. Conclusions

Many reports substantiate that by embedding Ag NPs in the cotton fabric, the fabric tends to show antibacterial activity. Also, binders are used to avoid detachment of Ag NPs during washing cycles. However, most of the used binders are either hydrophilic or toxic in nature. In this regard, the present study focused on developing antibacterial cotton fabric using

Ag NS embedded by PCL, a non-toxic, biodegradable, and hydrophobic polymer. The antibacterial test assessed using AATCC-147 and AATCC-100 shows that the Ag NS/PCL coated fabric releases the Ag^+ ions sustainably, showing slightly reduced antibacterial activity compared to the Ag NS coated cotton fabric. The durability test substantiates the significant reduction in Ag NS cotton fabrics' antibacterial activity due to the detachment of Ag NS. Ag NS/PCL modified fabric also displays a reduction in the activity, but not as significant as Ag NS modified fabric. Thus, Ag NS/PCL acts as a promising material for developing durable and sustained antibacterial fabrics.

In the present study, the prepared coating mixture contains a very low concentration of Ag moiety. Further, the dip coating technique introduces only a fraction of Ag moiety from the coating mixture over the fabric. The United States Environmental Protection Agency has set a secondary standard of 100 µg/L for maximum Ag intake per day [50]. Rationally thinking, the Ag moiety will be lower in the coated material than the set standard. Further, PCL is added as the biocompatible binder, which doesn't allow easy detachment of Ag NS from the coated fabric validated from the durability studies. However, future *in vitro* and *in vivo* toxicity studies are required to confirm these claims to make the coating mixture a commercially viable product. Future studies involve optimizing process parameters for the preparation of coating mixture to improve further the durability, analysis of cytotoxicity, and biocompatibility using *in-vitro* fibroblast cells and *in-vivo* small animal models.

Funding

This research was funded by the Life Science Research Board, Defence Research and Development Organisation, Ministry of Defence, Government of India, with grant number LSRB/01/15001/M/LSRB-371/LS&BD/2020.

Acknowledgments

The authors thank the management of Chettinad Academy of Research and Education for providing facilities to complete the research work successfully.

Conflicts of Interest

The authors declare no conflict of interest.

References

1. Syafiuddin, A. Toward a Comprehensive Understanding of Textiles Functionalized with Silver Nanoparticles. *J. Chinese Chem. Soc.* **2019**, *66*, 793–814, https://doi.org/10.1002/jccs.201800474.
2. Park, S.Y.; Chung, J.W.; Priestley, R.D.; Kwak, S.-Y. Covalent Assembly of Metal Nanoparticles on Cellulose Fabric and Its Antimicrobial Activity. *Cellulose* **2012**, *19*, 2141–2151, https://link.springer.com/article/10.1007/s10570-012-9773-6.
3. Broadhead, R.; Craeye, L.; Callewaert, C. The Future of Functional Clothing for an Improved Skin and Textile Microbiome Relationship. *Microorganisms* **2021**, *9*, 1192, https://doi.org/10.3390/microorganisms9061192.
4. Agrawal, N.; Low, P.S.; Tan, J.S.J.; Fong, E.W.M.; Lai, Y.; Chen, Z. Durable Easy-Cleaning and Antibacterial Cotton Fabrics Using Fluorine-Free Silane Coupling Agents and CuO Nanoparticles. *Nano Mater. Sci.* **2020**, *2*, 281–291, https://doi.org/10.1016/j.nanoms.2019.09.004.
5. İpek, Y.; Ertekin, Ö. Developing Antibacterial Cotton Fabric with Zinc Borate Impregnation Process. *Fibers Polym.* **2021**, *22*, 2826–2833, https://link.springer.com/article/10.1007/s12221-021-0670-1.
6. Román, L.E.; Gomez, E.D.; Solís, J.L.; Gómez, M.M. Antibacterial Cotton Fabric Functionalized with Copper Oxide Nanoparticles. *Molecules* **2020**, *25*, 5802, https://doi.org/10.3390/molecules25245802.
7. Nosheen, A.; Hussain, M.T.; Khalid, M.; Javid, A.; Aziz, H.; Iqbal, S.; Ashraf, M.; Ali, S. Development of

Protective Cotton Textiles against Biohazards and Harmful UV Radiation Using Eco-Friendly Novel Fiber-Reactive Bioactive Agent. *Process Saf. Environ. Prot.* **2022**, *165*, 431–444, https://doi.org/10.1016/j.psep.2022.07.035.
8. Riaz, S.; Ashraf, M.; Hussain, T.; Hussain, M.T.; Younus, A. Fabrication of Robust Multifaceted Textiles by Application of Functionalized TiO2 Nanoparticles. *Colloids Surfaces A Physicochem. Eng. Asp.* **2019**, *581*, 123799, https://doi.org/10.1016/j.colsurfa.2019.123799.
9. Abou Elmaaty, T.M.; Elsisi, H.; Elsayad, G.; Elhadad, H.; Plutino, M.R. Recent Advances in Functionalization of Cotton Fabrics with Nanotechnology. *Polymers (Basel).* **2022**, *14*, 4273, https://doi.org/10.3390/polym14204273.
10. El-Kheir, A.; El-Gabry, L.K. Potential Applications of Nanotechnology In Functionalization of Synthetic Fibres (A Review). *Egypt. J. Chem.* **2022**, *65*, 67–85, https://doi.org/10.21608/ejchem.2022.106369.4891.
11. Li, Y.; Zhang, W.; Niu, J.; Chen, Y. Mechanism of Photogenerated Reactive Oxygen Species and Correlation with the Antibacterial Properties of Engineered Metal-Oxide Nanoparticles. *ACS Nano* **2012**, *6*, 5164–5173, https://doi.org/10.1021/nn300934k.
12. Elwakil, B.H.; Toderas, M.; El-Khatib, M. Arc Discharge Rapid Synthesis of Engineered Copper Oxides Nano Shapes with Potent Antibacterial Activity against Multi-Drug Resistant Bacteria. *Sci. Rep.* **2022**, *12*, 1–10, https://www.nature.com/articles/s41598-022-24514-w.
13. Rai, M.K.; Deshmukh, S.D.; Ingle, A.P.; Gade, A.K. Silver Nanoparticles: The Powerful Nanoweapon against Multidrug-resistant Bacteria. *J. Appl. Microbiol.* **2012**, *112*, 841–852, https://doi.org/10.1111/j.1365-2672.2012.05253.x.
14. Younis, A.B.; Haddad, Y.; Kosaristanova, L.; Smerkova, K. Titanium Dioxide Nanoparticles: Recent Progress in Antimicrobial Applications. *Wiley Interdiscip. Rev. Nanomedicine Nanobiotechnology* **2022**, e1860, https://doi.org/10.1002/wnan.1860.
15. Talapko, J.; Matijević, T.; Juzbašić, M.; Antolović-Požgain, A.; Škrlec, I. Antibacterial Activity of Silver and Its Application in Dentistry, Cardiology and Dermatology. *Microorganisms* **2020**, *8*, 1400, https://doi.org/10.3390%2Fmicroorganisms8091400.
16. Bhardwaj, A.K.; Sundaram, S.; Yadav, K.K.; Srivastav, A.L. An Overview of Silver Nanoparticles as Promising Materials for Water Disinfection. *Environ. Technol. Innov.* **2021**, *23*, 101721, https://doi.org/10.1016/j.eti.2021.101721.
17. Jatoi, A.W.; Kim, I.S.; Ni, Q.Q. A Comparative Study on Synthesis of AgNPs on Cellulose Nanofibers by Thermal Treatment and DMF for Antibacterial Activities. *Mater. Sci. Eng. C* **2019**, *98*, 1179–1195, https://doi.org/10.1016/j.msec.2019.01.017.
18. Xu, L.; Yi-Yi, W.; Huang, J.; Chun-Yuan, C.; Zhen-Xing, W.; Xie, H. Silver Nanoparticles: Synthesis, Medical Applications and Biosafety. *Theranostics* **2020**, *10*, 8996, https://doi.org/10.7150%2Fthno.45413.
19. Godoy-Gallardo, M.; Eckhard, U.; Delgado, L.M.; de Roo Puente, Y.J.D.; Hoyos-Nogués, M.; Gil, F.J.; Perez, R.A. Antibacterial Approaches in Tissue Engineering Using Metal Ions and Nanoparticles: From Mechanisms to Applications. *Bioact. Mater.* **2021**, *6*, 4470–4490, https://doi.org/10.1016/j.bioactmat.2021.04.033.
20. Liu, W.; Wu, Y.; Wang, C.; Li, H.C.; Wang, T.; Liao, C.Y.; Cui, L.; Zhou, Q.F.; Yan, B.; Jiang, G.B. Impact of Silver Nanoparticles on Human Cells: Effect of Particle Size. *Nanotoxicology* **2010**, *4*, 319–330, https://doi.org/10.3109/17435390.2010.483745.
21. Slepička, P.; Slepičková Kasálková, N.; Siegel, J.; Kolská, Z.; Švorčík, V. Methods of Gold and Silver Nanoparticles Preparation. *Materials (Basel).* **2019**, *13*, 1, https://doi.org/10.3390%2Fma13010001.
22. Yang, Y.; Xu, S.; Xu, G.; Liu, R.; Xu, A.; Chen, S.; Wu, L. Effects of Ionic Strength on Physicochemical Properties and Toxicity of Silver Nanoparticles. *Sci. Total Environ.* **2019**, *647*, 1088–1096, https://doi.org/10.1016/j.scitotenv.2018.08.064.
23. Aadil, K.R.; Pandey, N.; Mussatto, S.I.; Jha, H. Green Synthesis of Silver Nanoparticles Using Acacia Lignin, Their Cytotoxicity, Catalytic, Metal Ion Sensing Capability and Antibacterial Activity. *J. Environ. Chem. Eng.* **2019**, *7*, 103296, https://doi.org/10.1016/j.jece.2019.103296.
24. Alharbi, N.S.; Alsubhi, N.S.; Felimban, A.I. Green Synthesis of Silver Nanoparticles Using Medicinal Plants: Characterization and Application. *J. Radiat. Res. Appl. Sci.* **2022**, *15*, 109–124, https://doi.org/10.1016/j.jrras.2022.06.012.
25. Eid, A.M.; Fouda, A.; Niedbała, G.; Hassan, S.E.-D.; Salem, S.S.; Abdo, A.M.; F Hetta, H.; Shaheen, T.I. Endophytic Streptomyces Laurentii Mediated Green Synthesis of Ag-NPs with Antibacterial and Anticancer Properties for Developing Functional Textile Fabric Properties. *Antibiotics* **2020**, *9*, 641, https://doi.org/10.3390/antibiotics9100641.
26. Shaheen, T.I.; Abd El Aty, A.A. In-Situ Green Myco-Synthesis of Silver Nanoparticles onto Cotton Fabrics for Broad Spectrum Antimicrobial Activity. *Int. J. Biol. Macromol.* **2018**, *118*, 2121–2130, https://doi.org/10.1016/j.ijbiomac.2018.07.062.
27. Tania, I.S.; Ali, M.; Azam, M. In-Situ Synthesis and Characterization of Silver Nanoparticle Decorated Cotton Knitted Fabric for Antibacterial Activity and Improved Dyeing Performance. *SN Appl. Sci.* **2019**, *1*, 1–9, https://link.springer.com/article/10.1007/s42452-018-0068-x.
28. Wibawa, P.J.; Nur, M.; Asy'ari, M.; Wijanarka, W.; Susanto, H.; Sutanto, H.; Nur, H. Green Synthesized

Silver Nanoparticles Immobilized on Activated Carbon Nanoparticles: Antibacterial Activity Enhancement Study and Its Application on Textiles Fabrics. *Molecules* **2021**, *26*, 3790, https://doi.org/10.3390%2Fmolecules26133790.
29. Zhu, J.; Li, H.; Wang, Y.; Wang, Y.; Yan, J. Preparation of Ag NPs and Its Multifunctional Finishing for Cotton Fabric. *Polymers (Basel).* **2021**, *13*, 1338, https://doi.org/10.3390%2Fpolym13081338.
30. Gao, Y.-N.; Wang, Y.; Yue, T.-N.; Weng, Y.-X.; Wang, M. Multifunctional Cotton Non-Woven Fabrics Coated with Silver Nanoparticles and Polymers for Antibacterial, Superhydrophobic and High Performance Microwave Shielding. *J. Colloid Interface Sci.* **2021**, *582*, 112–123, https://doi.org/10.1016/j.jcis.2020.08.037.
31. Rajendran, R.; Radhai, R.; Savitha, R.; Sundaram, S.K.; Kongarasi, K.; Geethadevi, C.; Rajalakshmi, V. A Study on the Antimicrobial Property of the Cotton Fabric Imparted with Michaelia Champaca Leaf Extract Loaded Nanoparticles. *Education* **2014**, *2015*.
32. Sadannavar, M.K.; Luo, Y.; Huang, J.; Cao, C.; Fan, C.; Manj, R.Z.A. Antibacterial Cotton Functionalized with Olive Oil for Developing Medical Textiles. *Indian J. Fibre Text. Res.* **2021**, *46*, 303–310, http://op.niscpr.res.in/index.php/IJFTR/article/view/38246.
33. Kahrilas, G.A.; Wally, L.M.; Fredrick, S.J.; Hiskey, M.; Prieto, A.L.; Owens, J.E. Microwave-Assisted Green Synthesis of Silver Nanoparticles Using Orange Peel Extract. *ACS Sustain. Chem. Eng.* **2014**, *2*, 367–376, https://doi.org/10.1021/sc4003664.
34. Shin, J.W.; Lim, H.-R.; Cho, H.-B.; Kwon, Y.-T.; Choa, Y.-H. Segregation-Controlled Self-Assembly of Silver Nanowire Networks Using a Template-Free Solution-Based Process. *Nanoscale* **2021**, *13*, 8442–8451, https://pubs.rsc.org/en/content/articlelanding/2021/nr/d0nr08762a.
35. Singh, V.; Shrivastava, A.; Wahi, N. Biosynthesis of Silver Nanoparticles by Plants Crude Extracts and Their Characterization Using UV, XRD, TEM and EDX. *African J. Biotechnol.* **2015**, *14*, 2554–2567, https://doi.org/10.5897/AJB2015.14692.
36. Naik, J.R.; David, M. Green Synthesis of Silver Nanoparticles Using Caesalpinia Bonducella Leaf Extract: Characterization and Evaluation of *in vitro* Anti-Inflammatory and Anti-Cancer Activities. *Inorg. Nano-Metal Chem.* **2022**, 1–11, https://doi.org/10.1080/24701556.2021.2025093.
37. Moghadas, M.R.S.; Motamedi, E.; Nasiri, J.; Naghavi, M.R.; Sabokdast, M. Proficient Dye Removal from Water Using Biogenic Silver Nanoparticles Prepared through Solid-State Synthetic Route. *Heliyon* **2020**, *6*, e04730, https://doi.org/10.1016/j.heliyon.2020.e04730.
38. Masum, M.M.I.; Siddiqa, M.M.; Ali, K.A.; Zhang, Y.; Abdallah, Y.; Ibrahim, E.; Qiu, W.; Yan, C.; Li, B. Biogenic Synthesis of Silver Nanoparticles Using Phyllanthus Emblica Fruit Extract and Its Inhibitory Action against the Pathogen Acidovorax Oryzae Strain RS-2 of Rice Bacterial Brown Stripe. *Front. Microbiol.* **2019**, *10*, 820, https://doi.org/10.3389/fmicb.2019.00820.
39. Jyoti, K.; Baunthiyal, M.; Singh, A. Characterization of Silver Nanoparticles Synthesized Using Urtica Dioica Linn. Leaves and Their Synergistic Effects with Antibiotics. *J. Radiat. Res. Appl. Sci.* **2016**, *9*, 217–227, https://doi.org/10.1016/j.jrras.2015.10.002.
40. Albeladi, S.S.R.; Malik, M.A.; Al-thabaiti, S.A. Facile Biofabrication of Silver Nanoparticles Using Salvia Officinalis Leaf Extract and Its Catalytic Activity towards Congo Red Dye Degradation. *J. Mater. Res. Technol.* **2020**, *9*, 10031–10044, https://doi.org/10.1016/j.jmrt.2020.06.074.
41. Prieto, P.; Nistor, V.; Nouneh, K.; Oyama, M.; Abd-Lefdil, M.; Díaz, R. XPS Study of Silver, Nickel and Bimetallic Silver–Nickel Nanoparticles Prepared by Seed-Mediated Growth. *Appl. Surf. Sci.* **2012**, *258*, 8807–8813, https://doi.org/10.1016/j.apsusc.2012.05.095.
42. Zanna, S.; Saulou, C.; Mercier-Bonin, M.; Despax, B.; Raynaud, P.; Seyeux, A.; Marcus, P. Ageing of Plasma-Mediated Coatings with Embedded Silver Nanoparticles on Stainless Steel: An XPS and ToF-SIMS Investigation. *Appl. Surf. Sci.* **2010**, *256*, 6499–6505, https://doi.org/10.1016/j.apsusc.2010.03.132.
43. Ramstedt, M.; Franklyn, P. Difficulties in Determining Valence for Ag0 Nanoparticles Using XPS—Characterization of Nanoparticles inside Poly (3-sulphopropyl Methacrylate) Brushes. *Surf. Interface Anal.* **2010**, *42*, 855–858, https://www.researchgate.net/publication/263738756_Difficulties_in_determining_valence_for_Ag0_nanoparticles_using_XPS_-_Characterization_of_nanoparticles_inside_poly_3-sulphopropyl_methacrylate_brushes.
44. Bhuyar, P.; Rahim, M.H.A.; Sundararaju, S.; Ramaraj, R.; Maniam, G.P.; Govindan, N. Synthesis of Silver Nanoparticles Using Marine Macroalgae Padina Sp. and Its Antibacterial Activity towards Pathogenic Bacteria. *Beni-Suef Univ. J. Basic Appl. Sci.* **2020**, *9*, 1–15, https://bjbas.springeropen.com/articles/10.1186/s43088-019-0031-y.
45. Huq, M.A. Green Synthesis of Silver Nanoparticles Using Pseudoduganella Eburnea MAHUQ-39 and Their Antimicrobial Mechanisms Investigation against Drug Resistant Human Pathogens. *Int. J. Mol. Sci.* **2020**, *21*, 1510, https://doi.org/10.3390/ijms21041510.
46. Andra, S.; Jeevanandam, J.; Muthalagu, M.; Danquah, M.K. Surface Cationization of Cellulose to Enhance Durable Antibacterial Finish in Phytosynthesized Silver Nanoparticle Treated Cotton Fabric. *Cellulose* **2021**, *28*, 5895–5910, https://link.springer.com/article/10.1007/s10570-021-03846-2.
47. Portella, E.H.; Romanzini, D.; Angrizani, C.C.; Amico, S.C.; Zattera, A.J. Influence of Stacking Sequence

on the Mechanical and Dynamic Mechanical Properties of Cotton/Glass Fiber Reinforced Polyester Composites. *Mater. Res.* **2016**, *19*, 542–547, https://www.scielo.br/j/mr/a/DX7BcTTbHxJjhw6y4LSLsMC/?lang=en.
48. Küçük, M.; Öveçoğlu, M.L. Fabrication of SiO2–ZnO NP/ZnO NR Hybrid Coated Cotton Fabrics: The Effect of ZnO NR Growth Time on Structural and UV Protection Characteristics. *Cellulose* **2020**, *27*, 1773–1793, https://link.springer.com/article/10.1007/s10570-019-02891-2.
49. Maghimaa, M.; Alharbi, S.A. Green Synthesis of Silver Nanoparticles from Curcuma Longa L. and Coating on the Cotton Fabrics for Antimicrobial Applications and Wound Healing Activity. *J. Photochem. Photobiol. B Biol.* **2020**, *204*, 111806, https://doi.org/10.1016/j.jphotobiol.2020.111806.
50. Organization, W.H. *Silver in Drinking Water: Background Document for Development of WHO Guidelines for Drinking-Water Quality*; World Health Organization, 2021, https://apps.who.int/iris/handle/10665/350935.

Supplementary materials

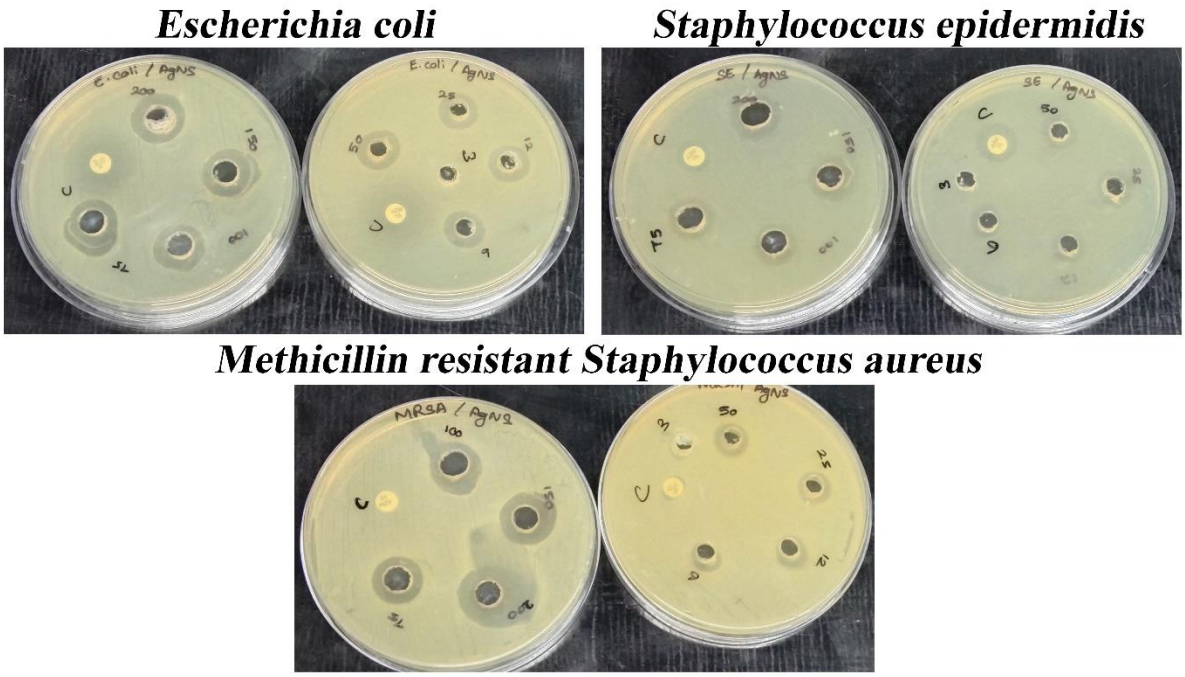

Figure S1. ZOI of Ag NS against *E. coli, S. epidermidis, and MRSA.*

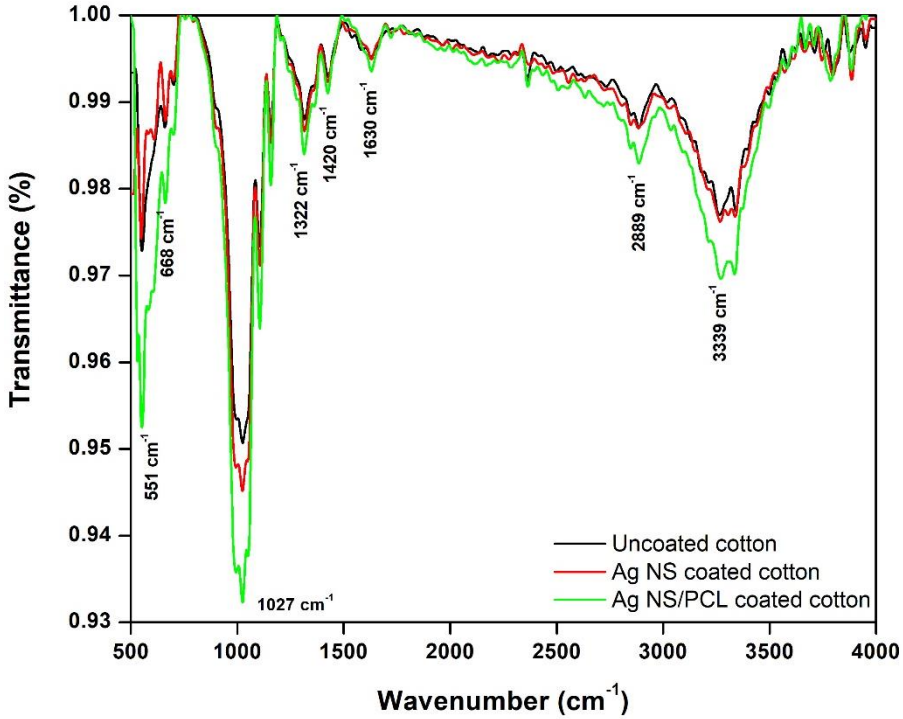

Figure S2. FTIR spectra of (**a**) uncoated, (**b**) Ag NS coated, and (**c**) Ag NS/PCL coated cotton fabrics

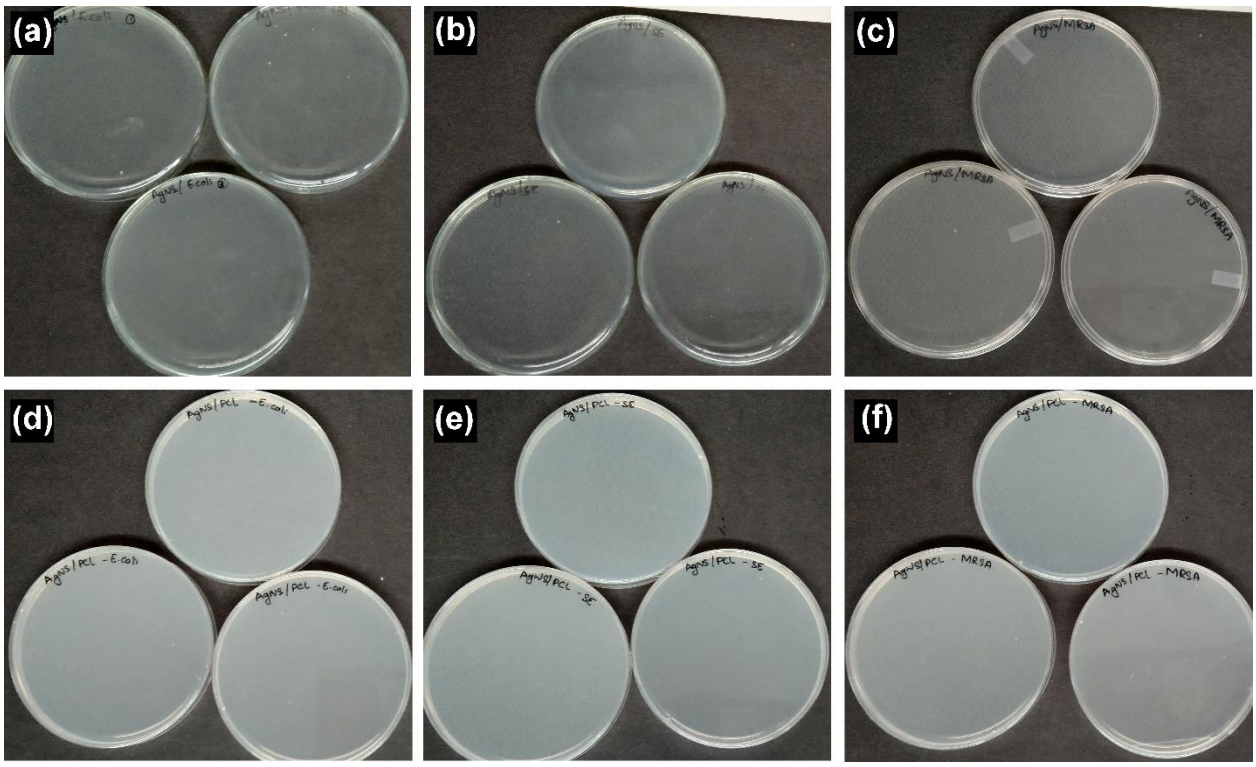

Figure S3. Colony counting plates of *E. coli, S. epidermidis, and MRSA* treated with (**a-c**) Ag NS and (**d-f**) Ag NS/PCL modified fabric.